Journal of Pioneering Medical Sciences
Received: February 23, 2026 | Accepted: September 14, 2026 | Published: November 05, 2026
Volume 15, Issue 10, Pages 141-155

DOI https://doi.org/10.47310/jpms2026151015



Repeated Sub-Inhibitory Antibiotic Exposure Drives a Partially Reversible, Multidimensional Adaptive Survival State in Clinical Multidrug-Resistant *Pseudomonas aeruginosa*

Reham A. Abd El Rahman[1*]
[1]Department of Clinical Laboratory Science, College of Applied Medical Sciences, University of Hafr Al-Batin (UHB), Hafr Al-Batin, Saudi Arabia

Author Designation: [1]Associate Professor

*Corresponding author: Dr. Reham A. Abd El Rahman (e-mail: raabdrahmen@uhb.edu.sa).

©2026 the Author(s). This is an open access article distributed under the terms of the Creative Commons Attribution License (http://creativecommons.org/licenses/by/4.0

Abstract Repeated exposure to sub-inhibitory antibiotic concentrations can alter bacterial killing dynamics without a corresponding change in the Minimum Inhibitory Concentration (MIC). It remains unclear to what extent biofilm remodelling, persister enrichment and efflux activation arise concurrently in clinical Multidrug-Resistant (MDR) *Pseudomonas aeruginosa*. We studied 48 clinical MDR *P. aeruginosa* isolates, each conditioned separately with ciprofloxacin, meropenem and tobramycin, yielding 144 isolate-antibiotic pairs assessed from baseline to Day 7. Endpoints comprised normalised growth, crystal-violet biofilm biomass, viable biofilm burden, high-resolution time-kill kinetics, MDK99 (the minimum duration required to kill 99% of the starting population), persister fraction, relative functional efflux index, pharmacological efflux inhibition, MIC reassessment, antibiotic-withdrawal recovery, cross-challenge and targeted *mexB*, *mexD*, *mexF* and *mexY* expression, analysed in linear mixed-effects models with the clinical isolate as the random effect. In all 144 pairs, the 1/4-MIC condition retained 86.1% of matched unexposed growth at Day 3 (normalised growth 0.861; 95% CI, 0.854-0.868) and produced non-monotonic biofilm remodelling (Day-7 biomass 1.127-fold versus matched 0-MIC controls; 1.079-1.177). The primary tolerance analysis was restricted to the 130 of 144 pairs (90.3%) without a two-fold or greater Day-3 MIC rise, the remaining 14 pairs being analysed separately as resistance-associated shifts. In these 130 pairs, MDK99 increased by 0.334 h at Day 3 (95% CI, 0.224-0.443) and 0.360 h at Day 7 (0.201-0.520), with median persister-fraction increases of 2.11- and 2.69-fold. Functional efflux rose in all 144 pairs (+0.217 index units at Day 3; 0.164-0.271). In a predefined subset of 24 isolates (72 pairs), efflux inhibition lowered survival of the bactericidal challenge, defined as the proportion of the starting inoculum recoverable at 8 h, by 13.34 absolute percentage points (95% CI, 11.03-15.66). Persister enrichment was the only independent predictor of the change in MDK99 ($\beta = 0.325$ h per 1-log10 increase; 95% CI, 0.129-0.522; FDR-adjusted $p = 0.00704$); the changes in efflux and biofilm were not. After antibiotic withdrawal in 72 pairs, MDK99, persister fraction, efflux and biofilm biomass all shifted significantly back toward baseline without full normalisation and 7 of 72 pairs retained a two-fold MIC elevation; generalised cross-tolerance was uncommon (mean cross-MDK fold change 1.038; range 0.720-1.365). Repeated non-lethal antibiotic stress therefore induced a multidimensional, only partially reversible survival state that MIC-defined susceptibility testing did not capture. As an *in vitro* study of a modest isolate collection, with recovery, microscopy and expression endpoints assessed in predefined subsets and without genomic analysis, these findings require validation in infection models before clinical inference.

Key Words *Pseudomonas aeruginosa*, Antibiotic Tolerance, Multidrug Resistance, Persister Cells, Biofilm, Efflux Pumps

INTRODUCTION

Conventional susceptibility testing does not fully explain why Multidrug-Resistant (MDR) *Pseudomonas aeruginosa* infections persist during chronic or spatially structured infection, nor why they are difficult to eradicate. Several mechanisms allow bacterial populations to survive otherwise lethal antibiotic exposure, including biofilm formation, metabolic heterogeneity, diffusion limitation and slowly killed subpopulations [1-3]. Distinguishing resistance, tolerance and persistence is therefore essential and these terms are used here as defined in the consensus statement of Balaban *et al.* [4]. Resistance is the inherited ability to grow at elevated antibiotic concentrations and is quantified by an increase in the Minimum Inhibitory Concentration (MIC). Tolerance is the ability of a whole population to survive bactericidal exposure for longer without any increase in MIC and is quantified by the time required to achieve a defined extent of killing, such as the minimum duration for killing 99% of the

population (MDK99). Persistence describes a transient, non-inherited, phenotypically tolerant subpopulation that survives bactericidal exposure far longer than the bulk population and is identified by biphasic killing together with a quantifiable late-surviving fraction. Persisters are therefore phenotypically tolerant rather than resistant: they do not grow at raised antibiotic concentrations and their enrichment leaves the MIC unchanged. Because these phenotypes are mechanistically distinct, an unchanged MIC does not imply unchanged killing.

Antibiotic exposure below the growth-inhibitory threshold is a biologically plausible driver of adaptation that MIC testing cannot detect. During treatment, bacterial populations frequently encounter sub-inhibitory concentrations, because biofilms impose concentration gradients and chronic-infection microenvironments distribute drug unevenly. Such concentrations are not biologically neutral. In *P. aeruginosa*, the identity, concentration and duration of sub-inhibitory exposure, together with strain background, can modify biofilm formation and virulence-associated physiology and can select subpopulations that overproduce efflux pumps, with the direction of effect depending on the antibiotic [5-8]. Reports of both enhanced and suppressed biofilm formation under partial antibiotic stress show that defining "sub-inhibitory" as an arbitrary fraction of the MIC is insufficient and that the exposure window should instead be validated experimentally against measured growth [9,10].

Three adaptive domains are individually well described and could plausibly arise together. Biofilm remodelling alters nutrient access, spatial organisation, matrix transport and the proportion of metabolically active cells, each of which can reduce antibiotic efficacy [11,12]. Persister enrichment increases the phenotypically tolerant fraction that survives bactericidal exposure [13-15]. Resistance-Nodulation-Division (RND) efflux systems reduce intracellular drug accumulation and contribute to adaptive survival: *MexXY-OprM* has been linked to aminoglycoside tolerance and low ciprofloxacin concentrations can select efflux-overproducing mutants [8,16]. Because gene expression and correlation alone cannot establish that efflux prolongs survival, functional transport activity and its pharmacological perturbation must be measured directly. A complete assessment therefore requires MIC, biofilm phenotype, functional efflux, killing dynamics and persistence to be measured in the same isolates under the same exposure protocol.

These domains have, however, mostly been studied in isolation, using laboratory strains, single antimicrobial classes, short exposure windows or designs that are not directly comparable [17-20]. Longitudinal studies of chronic infection show that tolerance can evolve along a trajectory distinct from MIC change [21,22]. It therefore remains unknown whether standardised repeated sub-MIC exposure generates a multidimensional survival state within the same clinical MDR isolates, whether the phenotype domains are statistically coupled or merely co-occur and whether altered killing resolves when antibiotic pressure is withdrawn or extends to a mechanistically distinct antimicrobial class.

We hypothesised that repeated sub-inhibitory exposure of clinical MDR *P. aeruginosa* remodels the biofilm phenotype, enriches persisters, increases functional efflux activity and prolongs killing and that these changes arise without a stable increase in MIC and are at least partly reversible. The primary outcome was the exposure-induced change in MDK99 among pairs without early MIC elevation and the primary hypothesis was that persister enrichment, rather than efflux or biofilm change, would independently predict it. Three objectives followed: to validate the dose- and time-dependent sub-inhibitory exposure window during ciprofloxacin, meropenem and tobramycin conditioning; to quantify the relationships among biofilm biomass, viable burden, killing kinetics, MDK99, persister abundance, functional efflux and targeted mex expression; and to determine whether the adaptive phenotype reverses after antibiotic withdrawal or extends to a mechanistically distinct cross-challenge. The paired, continuous design assumed no causal ordering among domains and pairs that developed MIC increases were retained and analysed separately as resistance-associated shifts rather than discarded.

METHODS

Study Design, Isolate Collection and Ethical Considerations

This study analysed 48 non-duplicate clinical isolates of Pseudomonas aeruginosa with a Multidrug-Resistant (MDR) phenotype, recovered from blood, wound, respiratory, urine and other clinical specimens submitted for routine diagnostic testing to the microbiology laboratory of the study institution. Isolates were collected consecutively and only the first isolate from each patient and infection episode was retained, so that each isolate represents one patient. Inclusion required laboratory confirmation of *P. aeruginosa*, an MDR phenotype and viability on subculture; isolates that failed to grow on subculture or that could not be confirmed to species level were excluded. Species identity was confirmed by routine automated biochemical identification in the diagnostic laboratory and verified phenotypically by characteristic colonial morphology, production of pyocyanin and pyoverdine pigments, a positive oxidase reaction and growth at 42°C. Multidrug resistance was defined as non-susceptibility to at least one agent in three or more antimicrobial classes [23] and the resistance-class count reported for each isolate is the number of antimicrobial classes to which that isolate was non-susceptible; susceptibility categories were assigned using the Clinical and Laboratory Standards Institute (CLSI) M100 performance standards current at the time of testing. The study used archived bacterial isolates only. There was no patient contact, no intervention and no access to identifying information: isolates were pseudonymised at the point of collection and no demographic, diagnostic, ward-level or other patient-identifying variable was available in the analysis dataset. Because the work was confined to surplus bacterial isolates already obtained during routine care, involved no patient contact or intervention and used no clinical data, it did not meet the definition of human-subjects research; neither individual informed consent nor review by a research ethics committee was therefore required. The study

was conducted in accordance with the principles of the Declaration of Helsinki and with institutional policy governing the secondary use of surplus diagnostic isolates. Each isolate received an Isolate_ID and each isolate-antibiotic combination a Pair_ID. Every isolate was tested against ciprofloxacin, meropenem and tobramycin, giving 144 isolate-antibiotic pairs from 48 isolates. The clinical isolate was the experimental unit throughout: the three antibiotic-specific pairs contributed by one isolate are repeated measures on that isolate rather than independent isolates and every inferential model accounted for this clustering (Section 2.9).

Species Confirmation, Antimicrobial Susceptibility and Baseline MDR Phenotype

Baseline MICs of ciprofloxacin, meropenem and tobramycin were determined for every isolate by broth microdilution in cation-adjusted Mueller-Hinton broth, performed and interpreted according to CLSI M100. Isolates were suspended to a 0.5 McFarland standard and diluted to a final inoculum of approximately 5×10^5 CFU/mL in flat-bottomed 96-well microtitre plates, which were incubated at 35±2°C in ambient air for 16-20 h; the MIC was read as the lowest concentration producing no visible growth. Each agent was tested across a doubling-dilution series from 0.0625 to 64 mg/L and every MIC in the collection fell within this range, so no value required censoring at the limits of the series. *P. aeruginosa* ATCC 27853 was included as the quality-control strain in every run and results were accepted only when its MICs fell within the CLSI acceptable ranges; runs failing quality control were repeated in full. Each isolate's own baseline MIC then served as the reference for sub-inhibitory conditioning and for the subsequent bactericidal challenge and all exposure concentrations are expressed as fractions of that isolate-specific and antibiotic-specific baseline MIC. The 0-MIC condition denotes the matched antibiotic-free control and not a measured MIC of zero. MIC was reassessed by the same method after conditioning on Days 3 and 7 and expressed as fold change from baseline on the two-fold doubling-dilution (log2) scale, so that one dilution step corresponds to a two-fold change. To prevent emerging MIC-defined resistance from being misread as tolerance, the primary phenotypic-tolerance population excluded any pair whose Day-3 MIC rose by one or more doubling dilutions, that is a two-fold or greater increase; pairs showing exactly a two-fold rise were therefore excluded. This left 130 of the 144 pairs as tolerance-eligible and the remaining 14 pairs were retained and analysed separately as resistance-associated susceptibility shifts. Baseline MIC and the baseline resistance-class count describe the resistance diversity of the collection and were used as covariates, not as substitutes for killing measurements.

Antibiotics and Longitudinal Sub-Inhibitory Exposure Model

Ciprofloxacin, meropenem and tobramycin were obtained from commercial suppliers as analytical-grade powders of known potency, reconstituted in the diluents specified by the manufacturer, sterilised by 0.22 µm filtration where required and stored at −80°C as single-use aliquots; working solutions were prepared fresh on each day of use. Each agent was applied at 0 (the antibiotic-free control), 1/8, 1/4 and 1/2 of the pair's baseline MIC, with the corresponding absolute concentration in mg/L calculated individually for every isolate-antibiotic pair. Conditioning was performed in cation-adjusted Mueller-Hinton broth in flat-bottomed 96-well polystyrene plates at a working volume of 200 µL per well, inoculated to approximately 5×105 CFU/mL from an overnight subculture and incubated at 35±2°C in ambient air under static conditions. To maintain the nominal exposure concentration across the 7-day protocol, cultures were passaged every 24 h by transferring a 1:100 dilution into fresh medium containing freshly prepared antibiotic at the same fraction of the baseline MIC. Phenotypes were sampled on Days 1, 3 and 7. Each fraction-by-time condition was tested in three independent biological replicates, defined as separate cultures initiated from separate overnight subcultures on separate days; replicate-level values were retained for quality control and condition means were used for analysis. A replicate was discarded, without imputation, if the matched antibiotic-free control failed to reach the expected growth density or if purity plating indicated contamination, so a condition mean could rest on two rather than three valid replicates; this applied to ten 1/4-MIC condition means. Growth was quantified as optical density at 600 nm after 24 h of incubation and normalised as the ratio of the exposed condition to the matched antibiotic-free control from the same isolate, antibiotic, day and run, so that 1.0 denotes control growth. The Day-3 1/4-MIC condition was defined a priori as the primary conditioning state because normalised growth confirmed that replication was largely maintained at this fraction, whereas 1/2 MIC produced substantially greater growth inhibition; 1/4-MIC exposure was continued to Day 7 to test the durability of the response. Exposure fractions were calculated throughout from the same isolate-specific baseline MIC, keeping Days 1, 3 and 7 directly comparable and growth normalisation was verified before any downstream phenotype change was attributed to non-lethal conditioning.

Quantification of Biofilm Adaptation

Biofilm response was quantified by two complementary endpoints, crystal-violet biomass and viable biofilm burden. Biofilms were established in flat-bottomed 96-well polystyrene plates in cation-adjusted Mueller-Hinton broth and incubated statically at 35±2°C for 24 h. Planktonic cells were removed and the wells were washed three times with sterile Phosphate-Buffered Saline (PBS), air-dried, fixed with 99% methanol for 15 min, stained with 0.1% (w/v) crystal violet for 15 min and washed until the rinse ran clear; bound dye was then solubilised in 33% (v/v) glacial acetic acid and absorbance read at 570 nm. Every plate included six sterile medium-only wells and the mean blank absorbance was subtracted from each reading before analysis.

Readings were obtained in three independent biological runs per isolate-antibiotic condition, summarised as the condition mean and expressed as fold change relative to the paired baseline biomass of the same isolate-antibiotic combination; baseline crystal-violet biomass was therefore measured separately for each of the 144 pairs rather than taken from an isolate-level average. Baseline biofilm category was assigned by the criteria of Stepanović *et al.* [24], referenced to a cut-off Optical Density (ODc) defined as the mean of the negative control plus three standard deviations: weak, ODc < OD ≤ 2×ODc; moderate, 2×ODc < OD ≤ 4×ODc; and strong, OD > 4×ODc. This classification yielded 14 weak, 24 moderate and 10 strong isolates. Viable biofilm-associated cells were enumerated separately as log10 Colony-Forming Units (CFU): washed biofilms were disrupted by scraping followed by 5 min of water-bath sonication and the resulting suspension was serially diluted ten-fold and plated on Mueller-Hinton agar for colony counting after 24 h at 35±2°C. This endpoint distinguishes change in stained matrix from change in viable cell number and counts were analysed on the log10 scale. Both endpoints were measured across the four MIC fractions on Days 1, 3 and 7 and the 1/4-MIC Day-3 and Day-7 states were carried forward into the tolerance, persistence, efflux and recovery analyses. In a predefined subset of 12 isolates (36 isolate-antibiotic pairs), quantitative Confocal Laser Scanning Microscopy (CLSM) provided biovolume (μm3/μm2) and mean thickness (μm) after staining with a fluorescent live/dead bacterial viability stain, with biovolume and mean thickness quantified from the confocal image stacks using dedicated biofilm image-analysis software. Missing or quality-control-failed microscopy readings were not imputed and no representative microscopy images are reported.

High-Resolution Killing Kinetics, Tolerance and Persister Quantification

Time-kill assays were performed at baseline and after 1/4-MIC conditioning to Day 3 and Day 7. Each isolate-antibiotic pair was challenged at five times its own baseline MIC in cation-adjusted Mueller-Hinton broth in glass tubes at a starting density of approximately 1×10^{8} CFU/mL and incubated at 35±2°C with shaking at 180 rpm. Samples were removed at 0, 1, 2, 4, 6 and 8 h in three independent biological replicates, washed once in sterile saline to remove antibiotic carryover, serially diluted ten-fold in saline and plated in duplicate on Mueller-Hinton agar, with colonies counted after 24 h at 35±2°C. The lower limit of quantification was 100 CFU/mL, equivalent to 2.0 log10 CFU/mL; no condition mean reached this limit within the 8-h window. Replicate-level log10 CFU/mL values were retained for quality control and condition means were used for trajectory analysis. MDK99 was defined as the minimum duration required to kill 99% of the starting population, that is the time to a 2-log10 reduction from the 0-h count and was obtained by linear interpolation of log10 CFU/mL against time between the two sampling points bracketing the 2-log10 threshold. A pair that did not reach a 2-log10 reduction within the 8-h window would have been right-censored at 8 h and reported as such; MDK99 was determinable in every pair of the analysed populations, so no observation was censored. Killing-rate parameters were estimated separately for a prespecified early phase (0-2 h) and late phase (4-8 h) as the negative slope of log10 CFU/mL against time and are reported throughout as positive killing-rate magnitudes in log10 CFU/mL per hour, so that a smaller value denotes slower killing. Killing was classified as biphasic when the late-phase rate fell to half or less of the early-phase rate within the same curve and a quantifiable late-surviving fraction was present, rather than by visual inspection of the trajectory. Persister fractions were measured experimentally at baseline, Day 3, Day 7 and, where available, after recovery and were defined as the ratio of the viable count surviving the 8-h bactericidal challenge to the 0-h count; they were log10-transformed for inference because they spanned several orders of magnitude. MDK99 was interpreted as population-level tolerance and the persister fraction as the size of the surviving phenotypically tolerant subpopulation. MDK99, the early- and late-phase killing rates and the persister fraction were analysed as separate outcomes and were never combined into a composite score.

Functional Efflux Activity and Mechanistic Inhibition

Functional efflux activity was measured at baseline and on Days 1, 3 and 7 of 1/4-MIC conditioning using an ethidium bromide efflux assay. Cells were washed and resuspended in PBS to an optical density at 600 nm of 0.3, loaded with ethidium bromide at 2 μg/mL in the presence of carbonyl cyanide m-chlorophenylhydrazone for 60 min at room temperature to maximise intracellular accumulation, washed free of extracellular dye and energised by the addition of glucose to 0.4% (w/v). Efflux was followed as the loss of fluorescence at 530 nm excitation and 600 nm emission over 10 min at 37°C in a microplate fluorimeter. The relative functional efflux index was calculated as the initial rate of fluorescence loss in the test condition divided by that of the matched baseline measurement of the same isolate-antibiotic pair, so that the paired baseline equals 1.0; both fold change and absolute change from baseline were derived. Measurements used three independent biological replicates and single quality-control-failed replicates were discarded without imputation. Efflux inhibition was tested in the Day-3 conditioned state in a predefined subset of 24 isolates (72 isolate-antibiotic pairs) using Phenylalanine-Arginine β-Naphthylamide (PAβN) at 25 mg/L, added 30 min before the bactericidal challenge and maintained throughout it at 35±2°C. Dimethyl sulfoxide was applied as the vehicle control at the same final concentration (0.5%, v/v) in all paired wells. An inhibitor-only control confirmed that PAβN at this concentration was itself sub-inhibitory and did not reduce viability in the absence of antibiotic. Conditioned and inhibitor-treated measurements were compared within the same pair. The biological endpoint was the reduction, in absolute percentage points, in survival of the standardised bactericidal challenge, survival being defined as the proportion of the 0-h inoculum recoverable at 8 h.

Because pharmacological efflux inhibitors are not fully specific and can act on membrane potential and other transport processes, this experiment is interpreted as functional perturbation evidence rather than proof of efflux specificity and this limitation is addressed in Section 4.4. Functional transport activity was treated as the primary efflux endpoint and targeted mex transcription as molecular corroboration rather than as a substitute for it. Longitudinal analyses used within-pair change from baseline, which reduces the influence of isolate-level differences in absolute efflux activity.

Phenotypic Stability, Reversibility and Cross-Tolerance

A predefined subset of 24 isolates (72 isolate-antibiotic pairs) underwent a standardised antibiotic-withdrawal recovery phase: after Day-3 conditioning, cultures were washed twice in sterile PBS to remove residual antibiotic and then propagated in antibiotic-free cation-adjusted Mueller-Hinton broth through three serial 24-h passages before reassessment. MIC, MDK99, functional efflux, biofilm fold change and persister fraction were measured at baseline, after Day-3 conditioning and after recovery, in order to separate reversible phenotypic adaptation from stable susceptibility change. The same subset was then cross-challenged using a fixed mapping of ciprofloxacin-conditioned to tobramycin, meropenem-conditioned to ciprofloxacin and tobramycin-conditioned to meropenem. The cross-challenge was applied directly after Day-3 conditioning, without an intervening washout, at five times the isolate's baseline MIC for the challenge antibiotic, using the same time-kill protocol and sampling schedule as in Section 2.5. The primary cross-challenge outcome was the cross-MDK fold change, calculated as the MDK99 of the conditioned pair against the challenge antibiotic divided by the MDK99 of the same pair against the same challenge antibiotic at baseline, so that 1.0 denotes no change. The protocol also recorded three secondary descriptive categories, "Not evident", "Borderline" and "Present", which were assigned by the investigator performing the assay at the time of recording. Because no prespecified numerical threshold separating these categories was defined, they are reported only as descriptive frequencies alongside the continuous cross-MDK distribution; no threshold was reverse-engineered from the observed values and no conclusion rests on the categories alone.

Targeted Molecular Corroboration of Adaptive States

Targeted qRT-PCR was performed in the same predefined subset of 12 isolates (36 isolate-antibiotic pairs) that underwent quantitative CLSM, which allowed molecular and architectural measurements to be compared within one experimental set. The RND efflux targets measured were mexB, mexD, mexF and mexY. Total RNA was extracted from mid-exponential-phase cultures using a column-based RNA purification kit with on-column RNase-free DNase I digestion, followed by a second solution-phase DNase treatment to eliminate residual genomic DNA. RNA quantity and purity were assessed spectrophotometrically and only preparations with an A260/A280 ratio of 1.8-2.1 and intact ribosomal bands on agarose electrophoresis were carried forward. One microgram of total RNA was reverse-transcribed with random hexamer priming at 42°C for 30 min, followed by enzyme inactivation at 95°C for 3 min. Quantitative PCR was performed in 20 µL reactions with SYBR Green chemistry on a real-time PCR system, using an initial denaturation at 95°C for 10 min followed by 40 cycles of 95°C for 15 s and 60°C for 60 s, with a dissociation-curve step at the end of each run to confirm a single amplification product. Primers for mexB, mexD, mexF, mexY and the reference gene were those described by Oh *et al.* [25]; their sequences and amplicon sizes are listed in Supplementary Table S1. The amplification efficiency of each assay was determined from ten-fold serial dilution standard curves and accepted only within the range 90-110%. The housekeeping gene rpsL served as the reference gene and its stability was confirmed by the absence of any significant change in raw Ct across baseline, Day 3 and Day 7. Every run included no-template and no-reverse-transcriptase controls, neither of which produced amplification. Expression was quantified in the comparative-Ct framework. For each gene, three independent biological replicates were measured at baseline and on Days 3 and 7 of 1/4-MIC conditioning, each in three technical replicates; technical replicates differing by more than 0.5 Ct were repeated and accepted technical replicates were averaged to a single Ct per biological replicate. ΔCt was calculated as the target Ct minus the reference-gene Ct within the same sample, ΔΔCt as the mean ΔCt of the conditioned state minus the mean baseline ΔCt of the same pair and fold change as $2^{-\Delta\Delta Ct}$. Statistical inference was performed on the ΔCt and ΔΔCt (log2) scale rather than on raw fold changes, which are not expected to be Gaussian, with the biological replicate as the unit of analysis. The eight gene-by-time comparisons formed one prespecified family for false-discovery-rate control. Expression change was interpreted as molecular corroboration of the functional efflux phenotype.

Statistical Analysis

The clinical isolate was the experimental unit. Each of the 48 isolates contributed three antibiotic-specific pairs, which are repeated measures on the same isolate rather than 144 independent isolates and every inferential model accounted for this clustering. Continuous outcomes are summarised as means with 95% Confidence Intervals (CIs) or as medians with Interquartile Ranges (IQRs) according to their distribution. Longitudinal comparisons used linear mixed-effects models fitted by restricted maximum likelihood with a Gaussian response and an identity link. The general form was outcome ~ antibiotic + exposure fraction + exposure duration + prespecified interactions, with a random intercept for Isolate_ID. The integrated determinant model for the change in MDK99 was ΔMDK99 ~ Δlog10 persister fraction + Δefflux + Δlog2 biofilm fold change + exposure duration + antibiotic + baseline log2 MIC, with a random intercept for Isolate_ID, fitted to 260 Day-3 and Day-7 observations from the 130 tolerance-eligible pairs across 48 isolates. Categorical predictors were treatment-coded with ciprofloxacin as the reference antibiotic and Day 3 as the reference exposure duration; the antibiotic term was assessed by an omnibus Wald test on 2 degrees of freedom, with pairwise contrasts reported

against ciprofloxacin. For ΔMDK99 the variance structure was compared between an isolate-only random intercept and a nested Pair_ID-within-Isolate_ID structure by likelihood-ratio test: adding the nested variance component did not improve fit (χ^2 = 0.412, 1 degree of freedom, p = 0.521) and the nested model also had the higher AIC (558.95 versus 557.37), so the more parsimonious isolate-only random-intercept model was retained. Model diagnostics comprised inspection of standardised residuals against fitted values for heteroscedasticity, normal quantile-quantile plots of residuals and random effects and assessment of influential isolates by refitting the model with each isolate omitted in turn; no material departure from model assumptions was identified. Persister fractions were analysed on the log10 scale, biofilm fold changes on the log2 scale and baseline MIC on the log2 doubling-dilution scale. Spearman rank correlations assessed associations between paired changes from baseline. Benjamini-Hochberg False-Discovery-Rate (FDR) correction was applied within three prespecified comparison families: the biofilm endpoints by time, the six predictors of the integrated ΔMDK99 model and the eight gene-by-time ΔΔCt comparisons. The Friedman test of the exposure-fraction gradient and the single prespecified recovery contrasts were not members of a correction family; both unadjusted and FDR-adjusted p values are reported wherever correction was applied. Missing and quality-control-failed observations were not imputed, so the affected condition means rest on the surviving replicates and denominators vary by assay; the denominator for every analysis is stated in Section 3.1. Analyses were performed in Python 3.13.5 with NumPy 2.3.5, SciPy 1.17.0 and statsmodels 0.14.6. A two-sided $p<0.05$ was considered statistically significant, after multiplicity adjustment where applicable.

RESULTS

Clinical Isolate Population and Baseline Antimicrobial Phenotype

The collection comprised 48 independent clinical isolates of MDR *P. aeruginosa*, yielding 144 isolate-antibiotic observations. Specimen origin was urine in 15 isolates (31.3%), wound in 12 (25.0%), respiratory in 10 (20.8%), blood in 8 (16.7%) and other sites in 3 (6.3%). Non-susceptibility extended to three antimicrobial classes in 22 isolates, four classes in 18 and five classes in 8. Baseline MICs spanned a wide range: ciprofloxacin 0.125-16 mg/L (median 4; IQR 1-5), meropenem 0.25-32 mg/L (median 8; IQR 2-16) and tobramycin 0.25-32 mg/L (median 4; IQR 2-8). Baseline crystal-violet optical density ranged from 0.134 to 1.724 (median 0.492), corresponding to 14 weak, 24 moderate and 10 strong biofilm phenotypes and baseline viable biofilm burden ranged from 6.329 to 7.586 log10 CFU (median 7.026), confirming substantial heterogeneity before conditioning. All summary values, ranges, medians and category counts reported here were recalculated directly from the isolate-level rows displayed in Table 1. Because every isolate was tested against all three antibiotics, antibiotic-specific estimates were obtained with clustering at the isolate level rather than by treating the 144 pair-level observations as independent clinical samples.

Analysis populations and denominators were as follows. The 48 isolates generated 144 isolate-antibiotic pairs. Exposure-window validation, biofilm biomass, viable biofilm burden, MIC transitions and functional efflux used all 144 pairs. The primary tolerance analyses of MDK99, killing-rate parameters and persister fractions used the 130 pairs (90.3%) without a two-fold or greater Day-3 MIC increase, while the 14 excluded pairs (9.7%) are reported separately as resistance-associated shifts; the integrated mixed-effects model used 260 Day-3 and Day-7 observations from those 130 pairs. Quantitative CLSM and qRT-PCR used the same predefined subset of 12 isolates (36 pairs). Efflux inhibition used a predefined subset of 24 isolates (72 pairs), as did the antibiotic-withdrawal recovery and cross-challenge experiments. Of those 72 cross-challenge observations, 64 were also tolerance-eligible, so the correlation between Day-3 ΔMDK99 and cross-MDK fold change rests on 64 pairs, whereas the cross-MDK distribution and the descriptive categories are reported for all 72. No observation was imputed and ten 1/4-MIC condition means rest on two rather than three valid biological replicates following a single quality-control failure.

Validation of the Sub-MIC Adaptive-Exposure Window

Across the 144 antibiotic-specific observations, aggregated at the level of the 48 isolates, growth inhibition increased monotonically with exposure fraction (Friedman χ^2 = 140.48, $p = 2.99\times10^{-30}$). At Day 3, mean normalised growth across the 144 pairs was 0.994 (95% CI, 0.987-1.001) at 0 MIC, 0.926 (0.920-0.932) at 1/8 MIC, 0.861 (0.854-0.868) at 1/4 MIC and 0.683 (0.676-0.690) at 1/2 MIC. At the isolate level, 1/4 MIC reduced normalised growth by 0.134 relative to the matched unexposed condition (95% CI, 0.122-0.145; $p = 2.87\times10^{-27}$), so that approximately 86% of control growth was retained. Mean 1/4-MIC normalised growth was stable across Days 1, 3 and 7 (0.859, 0.861 and 0.863), identifying Day-3 1/4 MIC as the primary non-lethal conditioning state and Day 7 as the extended-exposure condition. This stability, rather than nominal concentration alone, justified selecting the 1/4-MIC fraction for longitudinal comparison.

Repeated Sub-MIC Exposure Induces Heterogeneous Biofilm Adaptation

Repeated exposure produced a heterogeneous, non-uniform biofilm response. At 1/4 MIC, mean biomass fold change rose from 1.061 at Day 1 to 1.131 at Day 3 and 1.207 at Day 7. Modelled biomass at Day 3 was 1.095-fold that of matched 0-MIC conditions (95% CI, 1.048-1.144; $p = 4.85\times10^{-5}$; FDR-adjusted $p = 7.28\times10^{-5}$) and at Day 7 was 1.127-fold (1.079-1.177; $p = 8.82\times10^{-8}$; FDR-adjusted $p = 5.29\times10^{-7}$). By contrast, mean fold changes at 1/2 MIC were 0.930, 1.025 and 1.059 at Days 1, 3 and 7, showing that greater partial inhibition did not produce proportionally greater biomass. Across the 144 isolate-antibiotic observations, Day-3 responses at 1/4 MIC ranged from 0.626 to 1.986 and Day-7 responses from 0.492 to 2.652. The non-monotonic concentration pattern therefore distinguished adaptive remodelling from a simple dose-proportional biomass response and the viable-count endpoint confirmed that the longitudinal signal was not attributable to increased crystal-violet retention alone.

Table 1: Clinical and Microbiological Characteristics of the MDR *Pseudomonas aeruginosa* Isolate Collection

Isolate ID	Specimen	CIP MIC (mg/L)	MEM MIC (mg/L)	TOB MIC (mg/L)	Resistance classes, n	Baseline CV OD	Biofilm class	Baseline viable biofilm (log10 CFU)
MDR-PA-001	Blood	1	1	2	3	0.375	Weak	6.980
MDR-PA-002	Wound	0.125	16	32	4	0.504	Moderate	7.006
MDR-PA-003	Wound	0.25	0.5	4	3	1.393	Strong	7.023
MDR-PA-004	Urine	4	8	2	5	0.134	Weak	6.983
MDR-PA-005	Respiratory	0.5	2	16	3	0.425	Moderate	7.067
MDR-PA-006	Blood	0.5	16	1	3	0.649	Moderate	7.494
MDR-PA-007	Respiratory	2	32	16	3	0.415	Moderate	6.579
MDR-PA-008	Urine	8	16	2	3	0.408	Moderate	6.996
MDR-PA-009	Respiratory	16	4	8	5	0.606	Moderate	7.340
MDR-PA-010	Urine	4	4	32	4	0.406	Moderate	7.013
MDR-PA-011	Blood	0.125	4	0.25	4	1.257	Strong	6.775
MDR-PA-012	Respiratory	16	0.5	4	4	0.406	Moderate	6.444
MDR-PA-013	Blood	1	8	16	4	0.307	Weak	6.941
MDR-PA-014	Respiratory	0.25	32	4	5	0.399	Weak	7.059
MDR-PA-015	Other	8	8	32	4	0.696	Moderate	7.192
MDR-PA-016	Wound	2	16	4	4	0.515	Moderate	6.865
MDR-PA-017	Wound	0.5	8	0.5	4	0.732	Moderate	6.693
MDR-PA-018	Urine	4	1	0.5	3	0.414	Moderate	6.526
MDR-PA-019	Other	0.25	16	8	3	0.588	Moderate	6.731
MDR-PA-020	Urine	4	16	4	4	0.291	Weak	6.969
MDR-PA-021	Urine	2	8	8	3	0.230	Weak	6.728
MDR-PA-022	Wound	8	8	8	4	1.010	Strong	7.478
MDR-PA-023	Blood	4	32	4	4	0.369	Weak	7.107
MDR-PA-024	Urine	16	2	0.5	4	0.392	Weak	7.176
MDR-PA-025	Blood	4	8	8	3	1.124	Strong	6.922
MDR-PA-026	Wound	16	32	2	3	0.238	Weak	7.486
MDR-PA-027	Respiratory	1	8	16	3	1.701	Strong	7.364
MDR-PA-028	Urine	16	1	1	4	0.481	Moderate	6.800
MDR-PA-029	Urine	4	32	4	3	0.743	Moderate	6.965
MDR-PA-030	Wound	1	8	8	3	0.532	Moderate	7.037
MDR-PA-031	Blood	16	16	4	3	0.225	Weak	7.119
MDR-PA-032	Urine	8	16	8	3	0.751	Moderate	7.071
MDR-PA-033	Wound	0.5	16	1	5	0.502	Moderate	7.522
MDR-PA-034	Wound	4	16	8	4	0.312	Weak	6.859
MDR-PA-035	Respiratory	4	0.25	2	5	0.445	Moderate	7.586
MDR-PA-036	Wound	4	16	4	4	1.291	Strong	7.258
MDR-PA-037	Urine	4	8	8	3	0.213	Weak	7.028
MDR-PA-038	Wound	8	4	2	4	0.466	Moderate	6.869
MDR-PA-039	Urine	4	8	4	3	0.639	Moderate	7.585
MDR-PA-040	Respiratory	0.25	1	16	4	0.252	Weak	6.611
MDR-PA-041	Blood	2	1	0.5	5	1.085	Strong	7.048
MDR-PA-042	Respiratory	4	16	8	5	0.811	Moderate	7.048
MDR-PA-043	Urine	2	2	1	3	1.724	Strong	7.133
MDR-PA-044	Urine	8	4	16	5	0.273	Weak	6.329
MDR-PA-045	Urine	0.125	4	0.25	3	1.267	Strong	7.142
MDR-PA-046	Wound	4	8	32	4	0.926	Strong	6.740
MDR-PA-047	Other	1	1	1	3	0.517	Moderate	7.216
MDR-PA-048	Respiratory	4	0.25	32	3	0.429	Moderate	7.288

Abbreviations: CIP, Ciprofloxacin; MEM, Meropenem; TOB, Tobramycin; MIC, Minimum Inhibitory Concentration; CV, Crystal Violet; CFU, Colony-Forming Units. Each row represents one independent clinical isolate; MIC values are baseline measurements

Viable biofilm burden rose modestly but significantly relative to the 0-MIC condition, by 0.053 log10 CFU at Day 3 (95% CI, 0.030-0.077; $p = 8.58\times10^{-6}$) and 0.049 log10 CFU at Day 7 (0.025-0.072; $p = 4.77\times10^{-5}$). Change in biomass correlated with change in viable burden at Day 3 (Spearman $\rho = 0.532$, $p = 7.08\times10^{-12}$), although substantial divergence between the two endpoints remained. The Day-7 1/4-MIC biomass response was largest for meropenem (1.292-fold), followed by tobramycin (1.204-fold) and ciprofloxacin (1.125-fold), with no significant antibiotic-by-time interaction ($p = 0.336$). In the predefined 12-isolate subset (36 pairs), CLSM biovolume increased from Day 1 to Day 3 by 0.935 units (95% CI, 0.265-1.606; $p = 0.011$) while thickness did not change significantly ($p = 0.652$). Ten 1/4-MIC condition means rested on two biological replicates retained after a single quality-control failure and no value was imputed (Figure 1).

Sub-MIC Conditioning Increases Persister Formation and Prolongs Killing

The primary tolerance population comprised 130 isolate-antibiotic pairs from 48 isolates, after exclusion of the 14 of 144 pairs whose Day-3 MIC rose two-fold or more, which separates emerging MIC-defined resistance from phenotypic tolerance.

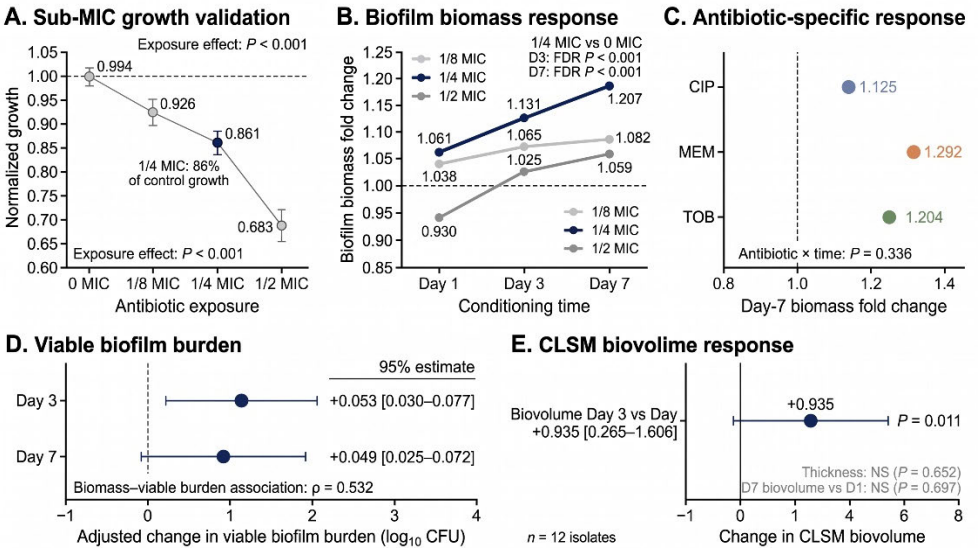


Figure 1: Dose-, Time- and Antibiotic-Dependent Biofilm Adaptation under the Validated sub-MIC Exposure Window. (A) Sub-MIC Growth Validation: Mean Normalised Growth with 95% CIs at 0, 1/8, 1/4 and 1/2 MIC on Day 3 across 144 Isolate–Antibiotic Observations from 48 Isolates, showing a Monotonic Exposure Effect (p<0.001) and Retention of 86% of Control Growth at 1/4 MIC. (B) Biofilm Biomass Response: Mean Biomass Fold Change at Days 1, 3 and 7 for the 1/8-, 1/4- and 1/2-MIC Conditions; the 1/4-MIC Condition Differed from the Matched 0-MIC Control at both Day 3 and Day 7 (FDR-adjusted p<0.001). (C) Antibiotic-Specific Response: Day-7 1/4-MIC Biomass fold Change for Ciprofloxacin (1.125), Meropenem (1.292) and Tobramycin (1.204), with no antibiotic × time interaction (p = 0.336). (D) Viable biofilm burden: adjusted change relative to the 0-MIC Condition at Day 3 (+0.053 log10 CFU; 95% CI, 0.030–0.077) and Day 7 (+0.049; 0.025–0.072), with the Biomass–Viable Burden Association (Spearman ρ = 0.532). (E) Quantitative CLSM Response in the Predefined 12-Isolate Subset (36 Isolate–Antibiotic Observations): Biovolume Increased from Day 1 to Day 3 (+0.935; 95% CI, 0.265–1.606; p = 0.011), whereas Thickness (p = 0.652) and Day-7 versus Day-1 Biovolume (p = 0.697) did not change significantly. CFU, Colony-Forming Units; CI, Confidence Interval; CLSM, Confocal Laser Scanning Microscopy; FDR, False-Discovery Rate; MIC, Minimum Inhibitory Concentration

Under the challenge at five times the baseline MIC, the mean viable count at baseline fell from 7.997 log10 CFU/mL at 0 h to 4.522 log10 CFU/mL at 8 h. More cells remained after 8 h in both conditioned states: the isolate-clustered mean difference was 0.340 log10 CFU/mL at Day 3 (95% CI, 0.213-0.468; $p = 1.68\times10^{-7}$) and 0.435 log10 CFU/mL at Day 7 (0.300-0.569; $p = 2.38\times10^{-10}$). Because the late phase slowed selectively while persister fractions rose, the kinetic change was concentrated in the surviving subpopulation rather than reflecting a general loss of initial bactericidal activity. Mean MDK99 increased from 2.613 h at baseline to 2.946 h at Day 3 and 2.976 h at Day 7, corresponding to increases of 0.334 h at Day 3 (95% CI, 0.224-0.443; $p = 2.17\times10^{-9}$) and 0.360 h at Day 7 (0.201-0.520; $p = 9.94\times10^{-6}$); median MDK99 fold change was 1.11 at Day 3 and 1.10 at Day 7. Killing-rate parameters are reported as positive killing-rate magnitudes, so that a smaller value denotes slower killing. Early-phase killing rates changed little (means 0.823, 0.853 and 0.878 log10 CFU/mL per hour at baseline, Day 3 and Day 7), whereas late-phase rates fell from 0.350 to 0.292 and 0.278 log10 CFU/mL per hour, making the slowly killed phase more prominent.

Persister enrichment accompanied the kinetic shift. The median persister fraction rose from 9.19×10^{-5} at baseline to 1.81×10^{-4} at Day 3 and 2.01×10^{-4} at Day 7. Isolate-clustered increases on the log10 scale were 0.336 at Day 3 (95% CI, 0.267-0.405; $p = 1.12\times10^{-21}$) and 0.439 at Day 7 (0.354-0.524; $p = 3.15\times10^{-24}$), equivalent to median fold increases of 2.11 and 2.69. Population-level tolerance, measured as MDK99 and the persistence-related late-surviving fraction therefore both increased while remaining analytically distinct outcomes (Figure 2).

Adaptive Survival is Accompanied by Functional Efflux Activation

Functional efflux increased after 1/4-MIC conditioning across all 144 isolate-antibiotic observations from 48 isolates. The mean relative efflux index rose from approximately 1.0 at baseline to 1.217 at Day 3 and 1.282 at Day 7, with estimated changes from baseline of +0.217 index units at Day 3 (95% CI, 0.164-0.271; $p = 1.32\times10^{-15}$) and +0.282 units at Day 7 (0.213-0.351; $p = 7.80\times10^{-16}$); the further increase from Day 3 to Day 7 was not significant (p = 0.056). The Day-7 index was highest for ciprofloxacin (1.386), followed by tobramycin (1.272) and meropenem (1.188). The inhibitor experiment demonstrated a functional contribution of efflux to survival even though the multivariable model reported below contained no independent Δefflux coefficient, which distinguishes perturbation evidence from population-level association.

In the predefined inhibitor subset (72 pairs from 24 isolates), mean Day-3 efflux fell from 1.217 to 0.784 and survival of the bactericidal challenge was reduced by 13.34 absolute percentage points (95% CI, 11.03-15.66).

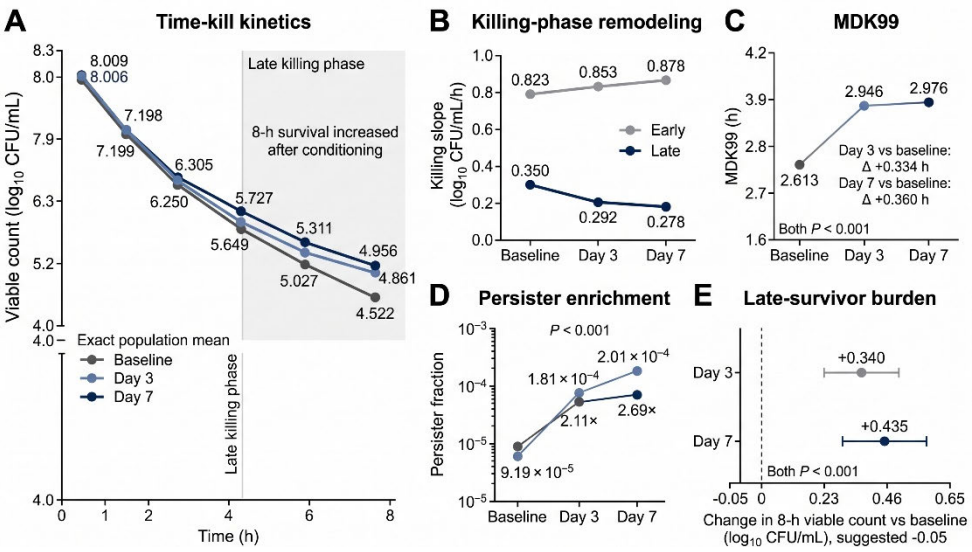


Figure 2: Sub-MIC Conditioning Reshapes Biphasic Killing Kinetics and Enriches Persister Populations, in the Primary tolerance-eligible population of 130 Isolate-Antibiotic Pairs from 48 Isolates. (A) Time-Kill Kinetics: Population mean Viable Counts Over 0–8 h under Challenge at Five Times the Baseline MIC at Baseline, Day 3 and Day 7, with the Prespecified Late Killing Phase Shaded; the 8-h Count rose from 4.522 log10 CFU/mL at Baseline to 4.861 at Day 3 and 4.956 at Day 7. (B) Killing-Phase Remodelling: Prespecified Early- and Late-Phase Killing Slopes at Baseline, Day 3 and Day 7, Reported as Positive Killing-Rate Magnitudes in log10 CFU/mL per hour, so that a Smaller Value Denotes Slower Killing; Early Slopes were 0.823, 0.853 and 0.878 and Late Slopes 0.350, 0.292 and 0.278. (C) MDK99 Rose from 2.613 h at Baseline to 2.946 h at Day 3 and 2.976 h at Day 7 (Δ +0.334 h and +0.360 h; both p<0.001). (D) Persister Enrichment: Median Persister Fraction of 9.19×10^{-5} at Baseline, 1.81×10^{-4} at Day 3 and 2.01×10^{-4} at Day 7, Equivalent to 2.11- and 2.69-Fold Increases (p<0.001). (E) Late-Survivor Burden: Change in the 8-h Viable Count Relative to Baseline, +0.340 log10 CFU/mL at Day 3 and +0.435 at Day 7 (both p<0.001). CFU, Colony-Forming Units; MDK99, Minimum Duration Required to Kill 99% of the Starting population; MIC, Minimum Inhibitory Concentration

In the molecular subset of 36 pairs from 12 isolates, Day-3 fold changes were 1.32 for *mexB*, 1.25 for *mexD*, 1.22 for *mexF* and 1.33 for *mexY* and the corresponding Day-7 fold changes were 1.26, 1.34, 1.22 and 1.25. All eight gene-by-time ΔΔCt comparisons remained significant after FDR correction (adjusted p≤0.0138). These expression changes corroborated the functional response but are not by themselves evidence of altered pump activity (Figure 3).

Increased Killing Tolerance Occurs without Equivalent Stable MIC Elevation and is Reversible

At Day 3, 130 of the 144 pairs (90.3%) retained their baseline MIC while 14 (9.7%) showed a two-fold or greater increase. By Day 7, MIC was unchanged in 100 of the 144 pairs (69.4%), two-fold higher in 35 (24.3%) and four-fold higher in 9 (6.3%), indicating that prolonged conditioning produced MIC-defined resistance in a minority of pairs, whereas early tolerance developed in most pairs without any MIC increase. Across all 144 pairs, ΔMDK99 at Day 3 was unrelated to the change in log2 MIC (Spearman ρ = 0.018, p = 0.827).

The recovery experiment assessed 72 isolate-antibiotic observations from the predefined subset of 24 isolates. Mean MDK99 fell from 3.029 h after Day-3 conditioning to 2.767 h after antibiotic withdrawal (mixed-effects change, –0.263 h; 95% CI, –0.391 to –0.134; $p = 6.05\times10^{-5}$), approaching but not reaching the baseline mean of 2.642 h for the same pairs. Functional efflux fell by 0.150 index units (95% CI, 0.105-0.196; $p = 9.17\times10^{-11}$), biofilm fold change by 0.103 units (0.056-0.151; $p = 2.33\times10^{-5}$) and the log10 persister fraction by 0.166 units (0.103-0.228; $p = 2.13\times10^{-7}$). Each endpoint therefore moved significantly toward baseline without returning to it and the recovery is accordingly described as partial rather than complete. Recovery MIC equalled baseline in 65 of the 72 pairs, whereas 7 pairs retained a two-fold elevation, confirming that a minority of pairs acquired a susceptibility change that did not reverse on withdrawal. In the cross-challenge, mean cross-MDK fold change was 1.038, with an observed range of 0.720-1.365 rather than a confidence interval (Figure 4E1) and the secondary descriptive categories were not evident in 54 of 72 observations, Borderline in 14 of 72 and Present in 4 of 72. Generalised cross-tolerance was therefore uncommon, although the continuous distribution shows that individual pairs varied in both directions; the categories are descriptive only and no conclusion rests upon them.

Integrated Determinants of the Adaptive Phenotype

Exposure-induced changes were selectively rather than universally coupled. At Day 3, change in biomass correlated with change in viable burden across all 144 pairs ($\rho = 0.532$, $p = 7.08\times10^{-12}$), whereas ΔMDK99 was unrelated to ΔMIC (ρ = 0.018, p = 0.827). Within the 130 tolerance-eligible pairs, ΔMDK99 correlated weakly with log10 persister enrichment (ρ = 0.189, p = 0.031) but not with Δefflux (ρ = –0.019, p = 0.834), log2 biofilm change (ρ = 0.101, p = 0.254) or change in viable burden (ρ = –0.043, p = 0.628).

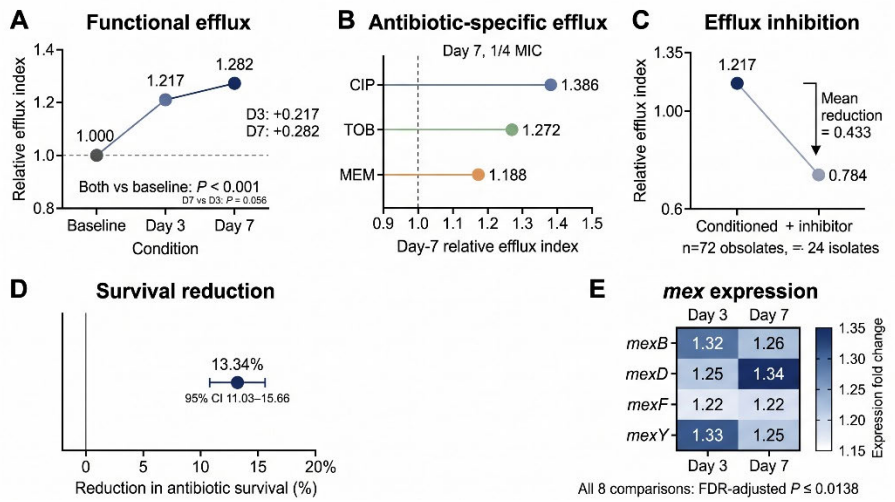


Figure 3: Functional Efflux Activation and Pharmacological Perturbation of Adaptive Survival. (A) Functional Efflux: the Relative Efflux Index Rose from 1.000 at Baseline to 1.217 at Day 3 and 1.282 at Day 7 across 144 Isolate-Antibiotic Observations from 48 Isolates (Δ +0.217 and +0.282; Both p<0.001), with the Further Day-7 Versus Day-3 Increase not Significant (p = 0.056). (B) Antibiotic-Specific Efflux: Day-7 Relative Efflux Index for Ciprofloxacin (1.386), Tobramycin (1.272) and Meropenem (1.188). (C) Efflux Inhibition in the Predefined 24-Isolate Subset (72 Isolate-Antibiotic Observations): the mean Day-3 Index Fell from 1.217 in the Conditioned State to 0.784 after Inhibitor Treatment, a Mean Reduction of 0.433 Index Units. (D) Survival Reduction: Efflux Inhibition Lowered Survival of the Bactericidal Challenge by 13.34 Absolute Percentage Points (95% CI, 11.03–15.66), Survival being the Proportion of the 0-h Inoculum Recoverable at 8 h. (E) Heatmap of *mexB*, *mexD*, *mexF* and *mexY* Expression fold Change at Day 3 and Day 7 in the Predefined 12-Isolate qRT-PCR Subset (36 Observations); All Eight Gene-by-Time Comparisons Remained Significant after FDR Correction (Adjusted p≤0.0138). Functional Efflux is the Primary Pump-Activity Endpoint and Expression is Molecular Corroboration. CI, Confidence Interval; FDR, False-Discovery Rate; qRT-PCR, Quantitative Reverse-Transcription Polymerase Chain Reaction

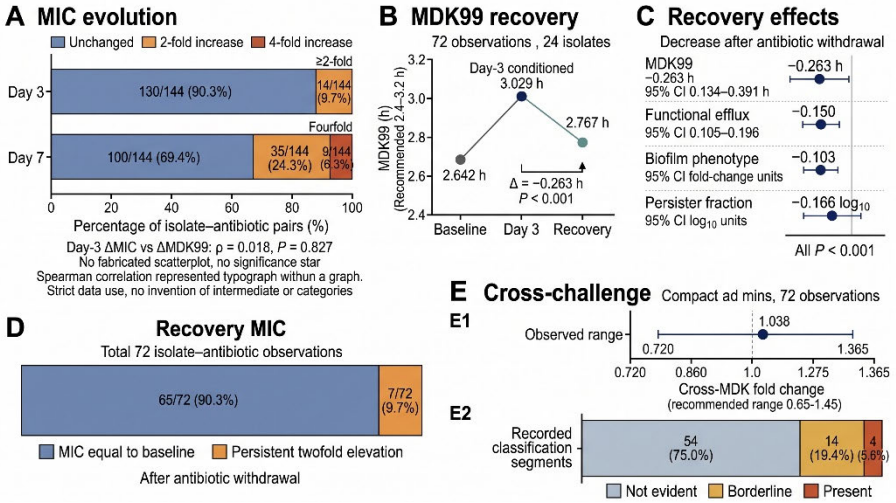


Figure 4: Dissociation of Killing Tolerance from MIC-Defined Resistance and Partial Reversibility after Antibiotic Withdrawal. (A) MIC Evolution Across all 144 Isolate–Antibiotic Pairs: at Day 3, 130 of 144 (90.3%) were Unchanged and 14 of 144 (9.7%) Rose Two-Fold or More; by Day 7, 100 of 144 (69.4%) were Unchanged, 35 of 144 (24.3%) had Risen two-fold and 9 of 144 (6.3%) Four-Fold. Day-3 ΔMIC was Unrelated to ΔMDK99 (Spearman ρ = 0.018, p = 0.827). (B) MDK99 Recovery in the Predefined 24-Isolate Subset (72 Observations): 2.642 h at Baseline, 3.029 h after Day-3 Conditioning and 2.767 h after Antibiotic Withdrawal (Δ −0.263 h; p<0.001). (C) Recovery Effects: Decrease after Withdrawal for MDK99 (-0.263 h; 95% CI, 0.134-0.391), Functional Efflux (–0.150; 0.105–0.196), Biofilm Phenotype (–0.103 fold-change units) and Persister Fraction (-0.166 log10 units); all p<0.001. (D) Recovery MIC across the Same 72 Observations: 65 of 72 Returned to the Baseline MIC while 7 of 72 Retained a Persistent Two-Fold Elevation. (E) Cross-Challenge in the same 72 Observations: (E1) Cross-MDK Fold Change, Mean 1.038 with an Observed Range of 0.720–1.365; (E2) the Recorded Descriptive Classifications, Not Evident in 54 (75.0%), Borderline in 14 (19.4%) and Present in 4 (5.6%), which are Descriptive Only. CI, Confidence Interval; MDK99, Minimum Duration Required to Kill 99% of the Starting Population; MIC, Minimum Inhibitory Concentration

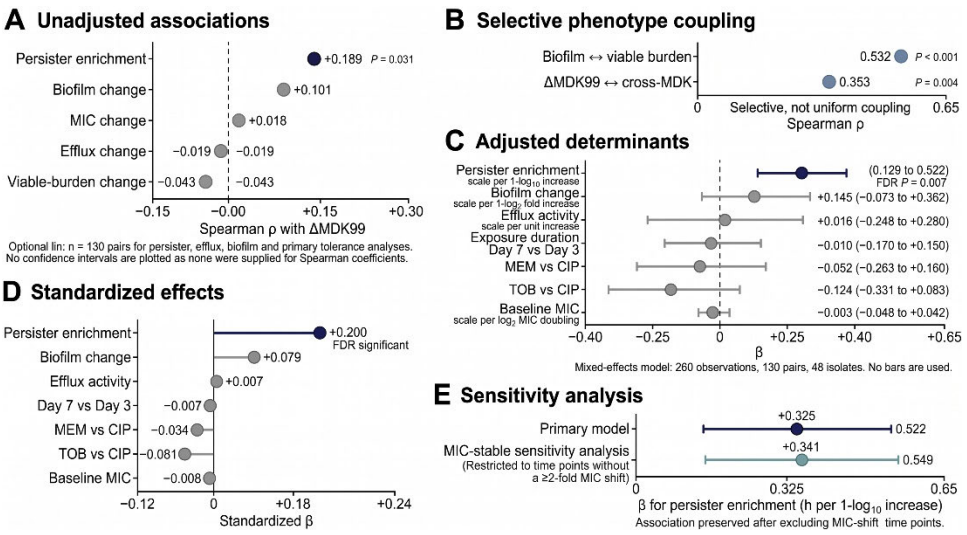


Figure 5: Integrated Determinants and Selective Coupling of the Multidimensional Adaptive Survival Phenotype. (A) Unadjusted Associations: Spearman ρ with ΔMDK99 for Persister Enrichment (+0.189; p = 0.031), Biofilm Change (+0.101), MIC change (+0.018), efflux change (−0.019) and viable-burden change (−0.043). (B) Selective phenotype Coupling: Biofilm Change Versus Viable Burden (ρ = 0.532; p<0.001) and ΔMDK99 versus cross-MDK fold change (ρ = 0.353; p = 0.004), Illustrating Selective Rather than Uniform Coupling. (C) Adjusted Determinants from the Mixed-Effects Model (260 Day-3 and Day-7 Observations, 130 Tolerance-Eligible Pairs, 48 Isolates): Persister Enrichment +0.325 h per 1-log10 Increase (95% CI, 0.129–0.522; FDR-Adjusted p = 0.007), Biofilm Change +0.145 (−0.073 to +0.362), Efflux Activity +0.016 (−0.248 to +0.280), Day 7 Versus Day 3 −0.010 (−0.170 to +0.150), Meropenem Versus Ciprofloxacin −0.052 (−0.263 to +0.160), Tobramycin Versus Ciprofloxacin −0.124 (−0.331 to +0.083) and Baseline MIC −0.003 per log2 Doubling (−0.048 to +0.042). (D) The Same Effects on the Standardized β Scale, with Persister Enrichment (+0.200) the Only FDR-Significant Predictor. (E) Sensitivity Analysis: The Persister Coefficient was Preserved when Analysis was Restricted to Time Points Without a Two-Fold or Greater MIC Shift (+0.341 Versus +0.325 in the Primary Model). Exposure Fraction was Fixed at 1/4 MIC in the Integrated Model. CI, Confidence Interval; FDR, False-Discovery Rate; MDK99, Minimum Duration Required to Kill 99% of the Starting Population; MIC, Minimum Inhibitory Concentration

Table 2: Multivariable Determinants of Sub-MIC-Induced Antibiotic Tolerance

Predictor	Adjusted β/effect	95% CI	Standardized β	P	FDR-adjusted P
Δ efflux activity	0.016 h per unit increase	−0.248 to 0.280	0.007	0.9058	0.9058
Δ persister fraction, log10	0.325 h per 1-log10 increase	0.129 to 0.522	0.200	0.00117	0.00704
Δ biofilm phenotype, log2 fold change	0.145 h per 1-log2 increase	−0.073 to 0.362	0.079	0.1925	0.5774
Exposure duration	Day 7 Vs Day 3: −0.010 h	−0.170 to 0.150	−0.007	0.9015	0.9058
Antibiotic	MEM Vs CIP: −0.052 h; TOB Vs CIP: −0.124 h	MEM: −0.263 to 0.160; TOB: −0.331 to 0.083	MEM: −0.034; TOB: −0.081	0.4933*	0.9058
Baseline MIC, log2	−0.003 h per MIC doubling	−0.048 to 0.042	−0.008	0.9029	0.9058

Among the 64 tolerance-eligible pairs that also had cross-challenge measurements, greater Day-3 ΔMDK99 was associated with greater cross-MDK fold change (ρ = 0.353, p = 0.00418).

The integrated longitudinal model included 260 Day-3 and Day-7 observations from the 130 tolerance-eligible pairs across 48 independent isolates. Adding a nested Pair_ID-within-Isolate_ID variance component to the isolate-only random intercept did not improve fit (χ^2 = 0.412, 1 degree of freedom, p = 0.521; AIC 558.95 for the nested model versus 557.37 for the isolate-only model), so the more parsimonious isolate-only model was retained. With exposure duration, antibiotic identity and baseline log2 MIC held constant, log10 persister enrichment independently predicted ΔMDK99 (β = 0.325 h per 1-log10 increase; 95% CI, 0.129-0.522; standardised β = 0.200; p = 0.00117; FDR-adjusted p = 0.00704). Neither Δefflux (β = 0.016; 95% CI, −0.248 to 0.280; p = 0.906) nor biofilm change (β = 0.145; −0.073 to 0.362; p = 0.192) was independently associated with ΔMDK99. ΔMDK99 was also independent of exposure duration (p = 0.901), antibiotic identity (omnibus Wald p = 0.493 on 2 degrees of freedom, with ciprofloxacin as the reference category) and baseline MIC (p = 0.903). A sensitivity analysis restricted to time points without a two-fold or greater MIC change retained the persister association (β = 0.341; 95% CI, 0.134-0.549; p = 0.00128) (Figure 5 and Table 2).

DISCUSSION

Principal Biological Finding

Repeated exposure to non-lethal antibiotic concentrations induced a survival phenotype in clinical MDR *P. aeruginosa*

that MIC testing did not capture. The most prominent dynamic signal was a prolonged MDK99, accompanied by enrichment of the late-surviving persister fraction, while 90.3% of isolate-antibiotic pairs retained their baseline MIC at Day 3. Biofilm remodelling and functional efflux activation occurred concurrently, but the integrated model did not support a uniformly coupled pathway: persister abundance was the only independent predictor of ΔMDK99, whereas Δefflux and Δbiofilm were not. Efflux nonetheless contributed functionally, because pharmacological inhibition reduced survival of the bactericidal challenge. That the early phenotype reverses only partially after withdrawal distinguishes it from stable resistance. This pattern is consistent with the resistance, tolerance and persistence framework of Balaban *et al.* [4] and with clinical studies showing that tolerance trajectories can diverge from conventional susceptibility change over time [21,26]. Mechanistically, the selective coupling matters, because co-occurrence alone does not establish an ordered causal pathway; the inhibitor experiment provides the most direct functional evidence of efflux involvement, within the limits set out below.

Biofilm Adaptation under Sub-MIC Exposure

Biofilm responses were neither uniformly positive nor uniform in direction. The clearest monotonic increase in biomass occurred at 1/4 MIC, whereas 1/2 MIC produced stronger early inhibition and no proportional response. This reconciles apparently conflicting reports that sub-inhibitory antibiotics either promote or suppress *P. aeruginosa* biofilm formation depending on the drug, the concentration, the strain background and the exposure history [7,9,10]. A separate viable-count endpoint was essential, because crystal violet stains matrix as well as cells. The correlation between biomass and viable burden indicates biological concordance, while the residual divergence confirms that matrix accumulation and viable population size are not interchangeable. Quantitative CLSM showed a short-term increase in biovolume without a concurrent increase in thickness, which points to architectural reorganisation rather than simple proportional growth. Biofilm tolerance can arise through diffusion limitation, metabolic state, matrix composition, spatial arrangement and aggregate physiology [1,17,18,27,28] and cellular arrangement and metabolic heterogeneity can further modulate local antibiotic susceptibility [11,12].

Persister Enrichment and Phenotypic Tolerance

The principal mechanistic difference lay in killing dynamics rather than growth inhibition. MDK99 increased in both conditioned states even though most pairs showed no MIC change at Day 3, which illustrates directly why MIC and killing duration describe distinct phenotypes. Following Balaban *et al.* [4], an increased MDK99 indicates population-level tolerance, whereas persistence requires a distinct slowly killed subpopulation. The present time-kill profiles support both: early killing was largely unchanged, late killing slowed and the persister fraction increased several-fold. Comparable late-survivor behaviour is seen in both planktonic and biofilm *P. aeruginosa*, although its magnitude depends strongly on the experimental system and conditions [13,20,29]. The association between log10 persister abundance and ΔMDK99, which persisted after adjustment and in the MIC-restricted sensitivity analysis, indicates that persistence-related variability most closely tracks prolonged killing in this dataset. In vitro persistence has been reported to reflect *in vivo* antibiotic survival of natural isolates [14] and intracellular or chronic infection niches may sustain populations that are difficult to eradicate [30]. These *in vitro* findings do not demonstrate treatment failure, but they do identify a plausible mechanism by which an unchanged MIC could coexist with slower bacterial clearance.

Efflux as a Functional Contributor to the Adaptive Phenotype

Functional efflux activity increased after conditioning, accompanied by modest increases in *mexB*, *mexD*, *mexF* and *mexY* expression. Efflux change did not, however, independently predict ΔMDK99. This dissociation is informative rather than contradictory: between-isolate variation in killing duration was not principally explained by efflux. Efflux activity in clinical MDR isolates is frequently heterogeneous [22] and has been linked to aminoglycoside tolerance and to adaptive susceptibility change [16,31]. Low ciprofloxacin concentrations can select efflux-overproducing subpopulations and altered regulation of efflux systems can shift the balance between resistance, tissue adaptation and tolerance [8,32]. The inhibition experiment provides functional rather than transcriptional evidence, since reduced efflux activity was accompanied by reduced antibiotic survival and multidrug transport systems have elsewhere been shown to contribute to reduced antibiotic susceptibility [33]. This result must nevertheless be interpreted cautiously. Pharmacological efflux inhibitors are not fully specific: agents of this class can perturb membrane potential, the proton-motive force and other transport processes, so part of the observed reduction in survival may not be attributable to efflux inhibition alone. No genetic complementation or pump-deletion control was performed here. The inhibitor data therefore support a functional contribution of efflux to the adaptive phenotype but do not establish efflux as the cause of the overall adaptive state, a conclusion reinforced by the null adjusted association between Δefflux and ΔMDK99.

Multidimensional Adaptation and Clinical Significance

The exposure response is best described as multidimensional rather than uniformly coordinated. Biofilm remodelling, persister enrichment, efflux activation and delayed killing occurred concurrently, yet statistical coupling was selective. Persister enrichment was the only independent predictor of prolonged MDK99. Efflux activation accompanied the adaptive state and was functionally implicated by the inhibitor experiment, but showed no independent association with MDK99 in the adjusted model and biofilm change

likewise co-occurred without independently explaining MDK99. The absence of a ΔMIC-ΔMDK99 association, together with the partial return of several phenotypes after antibiotic withdrawal, supports a substantial reversible component. Generalised cross-tolerance was uncommon, although the association between Day-3 ΔMDK99 and continuous cross-MDK fold change indicates that some pairs developed broader survival effects. In the clinic, antimicrobial pharmacodynamics can be modified by biofilm penetration gradients, chronic infection niches, variable tissue concentrations and nutrient conditions [3,34]. These findings are generated *in vitro* from clinical isolates and are not patient-outcome data: they do not demonstrate clinical treatment failure and do not by themselves establish a treatment strategy. They do, however, generate the testable hypothesis that limiting prolonged subtherapeutic exposure may matter for both short-term bacterial survival and longer-term resistance selection, in a way that routine MIC testing would not detect; that hypothesis requires validation in infection models and clinical studies before it can inform practice. The recovery data add a further dimension: the partial return of several traits after withdrawal is consistent with regulatory, reversible adaptation, whereas the subset of pairs retaining MIC increases indicates that a stable susceptibility change also occurred in a minority of pairs.

Strengths, Limitations and Next Mechanistic Steps

The strengths of this design include longitudinal assessment of 48 clinical MDR isolates against three antibiotic classes, multiple sub-MIC fractions, paired longitudinal conditioning, high-resolution time-kill trajectories, both viable and biomass biofilm endpoints, MDK99 and persister measurement, functional efflux with pharmacological perturbation, recovery and cross-challenge phases, targeted qRT-PCR corroboration and mixed-effects analysis that preserves the clinical isolate as the independent experimental unit. Several limitations qualify the findings. First, the isolate collection is modest: 48 isolates from a single collection give limited power to detect small effects and limited ability to characterise uncommon phenotypes and the 144 pairs are repeated measures on those 48 isolates rather than independent observations. Second, the microscopy, qRT-PCR, efflux-inhibition, recovery and cross-challenge experiments were performed in predefined subsets of 12 or 24 isolates, so those estimates are less precise than the full-collection analyses and were not designed to support subgroup comparison. Third, generalisability across settings is uncertain, because the isolates derive from a single institution and collection period and local resistance epidemiology and clonal structure may differ elsewhere. Fourth, repeated sub-MIC exposure can select pre-existing resistant or efflux-overproducing subpopulations as well as induce reversible physiological adaptation; these two processes are not separated in the present design and the pairs that developed stable MIC increases are consistent with such selection. Fifth, no genomic analysis was performed, so mutation-driven change cannot be distinguished from phenotypic or regulatory adaptation; whole-genome sequencing of baseline, conditioned and recovered populations would be required for that purpose. Sixth, the 8-hour killing observation window, although sufficient to determine MDK99 in the analysed pairs, cannot characterise later killing phases or very slowly dividing survivors and the 7-day conditioning protocol is considerably shorter than clinically relevant chronic exposure. Seventh, pharmacological efflux inhibition lacks genetic specificity controls, as discussed in Section 4.4. Finally, the descriptive cross-tolerance categories lack documented operational thresholds and are therefore reported only alongside the continuous outcome. Future work should combine whole-genome sequencing with transcriptomics, proteomics, metabolomics, c-di-GMP measurement and infection-model validation to establish whether reversible tolerance predicts treatment persistence *in vivo* [35] and should separate regulatory adaptation from mutation-driven evolution. Translational studies should accordingly report dynamic killing endpoints alongside conventional susceptibility data rather than relying on either alone.

CONCLUSION

Repeated exposure of clinical MDR *Pseudomonas aeruginosa* to sub-inhibitory concentrations of ciprofloxacin, meropenem and tobramycin was biologically active and produced changes in survival that MIC testing alone did not capture. Conditioning produced heterogeneous biofilm remodelling, a modest increase in viable biofilm burden, persister enrichment, functional efflux activation and prolonged MDK99. The clearest early signal appeared in the isolate-antibiotic pairs that retained their baseline MIC at Day 3. Persister enrichment independently predicted ΔMDK99, whereas changes in efflux and biofilm showed no independent statistical association with killing duration; efflux inhibition nonetheless reduced antibiotic survival, indicating a functional contribution to the adaptive phenotype that the association analysis alone did not reveal. The absence of any association between ΔMIC and ΔMDK99 further separates conventional resistance from killing tolerance. After antibiotic withdrawal, MDK99, persister fraction, efflux activity and biofilm phenotype all moved significantly toward baseline but did not fully normalise and 7 of 72 pairs retained a two-fold MIC elevation, so the phenotype is partially rather than wholly reversible. Cross-tolerance was uncommon, indicating that adaptation was largely but not exclusively specific to the conditioning antibiotic, since a minority of pairs did show cross-challenge changes whose magnitude correlated with the degree of conditioned tolerance. Repeated non-lethal antibiotic stress therefore produces a multidimensional, selectively coupled and only partially reversible survival state. These *in vitro* findings suggest, as a hypothesis for further testing, that limiting prolonged subtherapeutic exposure may be important in infection settings where tissue pharmacokinetics, biofilm structure or spatial gradients expose bacterial populations to non-lethal drug concentrations and they show that dynamic killing endpoints convey information that conventional MIC testing does not.

REFERENCES

[1] Ciofu, O. and T. Tolker-Nielsen. "Tolerance and resistance of *Pseudomonas aeruginosa* biofilms to antimicrobial agents-How *P. aeruginosa* can escape antibiotics." *Frontiers in Microbiology*, vol. 10, 2019, article 913. DOI: 10.3389/fmicb.2019.00913

[2] Fernández-Billón, M. *et al.* "Mechanisms of antibiotic resistance in *Pseudomonas aeruginosa* biofilms." *Biofilm*, vol. 5, 2023, article 100129. DOI: 10.1016/j.bioflm.2023.100129.

[3] Stewart, P.S. *et al.* "Conceptual model of biofilm antibiotic tolerance that integrates phenomena of diffusion, metabolism, gene expression and physiology." *Journal of Bacteriology*, vol. 201, no. 22, 2019, article e00307-19. DOI: 10.1128/JB.00307-19.

[4] Balaban, N.Q. *et al.* "Definitions and guidelines for research on antibiotic persistence." *Nature Reviews Microbiology*, vol. 17, no. 7, 2019, pp. 441-448. DOI: 10.1038/s41579-019-0196-3.

[5] Ahmed, M.N. *et al.* "Evolution of antibiotic resistance in biofilm and planktonic *Pseudomonas aeruginosa* populations exposed to subinhibitory levels of ciprofloxacin." *Antimicrobial Agents and Chemotherapy*, vol. 62, no. 8, 2018, article e00320-18. DOI: 10.1128/AAC.00320-18.

[6] Nolan, C. and V. Behrends. "Sub-inhibitory antibiotic exposure and virulence in *Pseudomonas aeruginosa*." *Antibiotics*, vol. 10, no. 11, 2021, article 1393. DOI: 10.3390/antibiotics10111393.

[7] Otani, S. *et al.* "Sub-minimum inhibitory concentrations of ceftazidime inhibit *Pseudomonas aeruginosa* biofilm formation." *Journal of Infection and Chemotherapy*, vol. 24, no. 6, 2018, pp. 428-433. DOI: 10.1016/j.jiac.2018.01.007.

[8] Sanz-García, F. *et al.* "Low ciprofloxacin concentrations select multidrug-resistant mutants overproducing efflux pumps in clinical isolates of *Pseudomonas aeruginosa*." *Microbiology Spectrum*, vol. 10, no. 5, 2022, article e00723-22. DOI: 10.1128/spectrum.00723-22.

[9] Hagras, S.A.A. *et al.* "Effect of sub-inhibitory concentrations of cefepime on biofilm formation by *Pseudomonas aeruginosa*." *Canadian Journal of Microbiology*, vol. 67, no. 12, 2021, pp. 894-901. DOI: 10.1139/cjm-2021-0229.

[10] Khan, F. *et al.* "Inhibition of biofilm and virulence properties of *Pseudomonas aeruginosa* by sub-inhibitory concentrations of aminoglycosides." *Microbial Pathogenesis*, vol. 146, 2020, article 104249. DOI: 10.1016/j.micpath.2020.104249.

[11] Dayton, H. *et al.* "Cellular arrangement impacts metabolic activity and antibiotic tolerance in *Pseudomonas aeruginosa* biofilms." *PLOS Biology*, vol. 22, no. 2, 2024, article e3002205. DOI: 10.1371/journal.pbio.3002205.

[12] Schiessl, K.T. *et al.* "Phenazine production promotes antibiotic tolerance and metabolic heterogeneity in *Pseudomonas aeruginosa* biofilms." *Nature Communications*, vol. 10, 2019, article 762. DOI: 10.1038/s41467-019-08733-w.

[13] Patel, H. *et al.* "*Pseudomonas aeruginosa* persister cell formation upon antibiotic exposure in planktonic and biofilm state." *Scientific Reports*, vol. 12, 2022, article 16151. DOI: 10.1038/s41598-022-20323-3.

[14] Verstraete, L. *et al.* "In vitro persistence level reflects *in vivo* antibiotic survival of natural *Pseudomonas aeruginosa* isolates in a murine lung infection model." *Microbiology Spectrum*, vol. 11, no. 3, 2023, article e04970-22. DOI: 10.1128/spectrum.04970-22.

[15] Zhu, K. *et al.* "Universal antibiotic tolerance arising from antibiotic-triggered accumulation of pyocyanin in *Pseudomonas aeruginosa*." *PLOS Biology*, vol. 17, no. 12, 2019, article e3000573. DOI: 10.1371/journal.pbio.3000573.

[16] Fan, Z. *et al.* "*Pseudomonas aeruginosa* polynucleotide phosphorylase controls tolerance to aminoglycoside antibiotics by regulating the MexXY multidrug efflux pump." *Antimicrobial Agents and Chemotherapy*, vol. 65, no. 2, 2021, article e01846-20. DOI: 10.1128/AAC.01846-20.

[17] Poudyal, B. and K. Sauer. "The ABC of biofilm drug tolerance: The MerR-like regulator BrlR is an activator of ABC transport systems, with PA1874-77 contributing to the tolerance of *Pseudomonas aeruginosa* biofilms to tobramycin." *Antimicrobial Agents and Chemotherapy*, vol. 62, no. 2, 2018a, article e01981-17. DOI: 10.1128/AAC.01981-17.

[18] Poudyal, B. and K. Sauer. "The PA3177 gene encodes an active diguanylate cyclase that contributes to biofilm antimicrobial tolerance but not biofilm formation by *Pseudomonas aeruginosa*." *Antimicrobial Agents and Chemotherapy*, vol. 62, no. 10, 2018b, article e01049-18. DOI: 10.1128/AAC.01049-18.

[19] Thöming, J.G. and S. Häussler. "*Pseudomonas aeruginosa* is more tolerant under biofilm than under planktonic growth conditions: A multi-isolate survey." *Frontiers in Cellular and Infection Microbiology*, vol. 12, 2022, article 851784. DOI: 10.3389/fcimb.2022.851784.

[20] Žiemytė, M. *et al.* "Real-time monitoring of *Pseudomonas aeruginosa* biofilm growth dynamics and persister cells' eradication." *Emerging Microbes & Infections*, vol. 10, no. 1, 2021, pp. 2062-2075. DOI: 10.1080/22221751.2021.1994355.

[21] Ghoul, M. *et al.* "Long-term evolution of antibiotic tolerance in *Pseudomonas aeruginosa* lung infections." *Evolution Letters*, vol. 7, no. 6, 2023, pp. 389-400. DOI: 10.1093/evlett/qrad034.

[22] Ugwuanyi, F.C. *et al.* "Evaluation of efflux pump activity and biofilm formation in multidrug resistant clinical isolates of *Pseudomonas aeruginosa* isolated from a Federal Medical Center in Nigeria." *Annals of Clinical Microbiology and Antimicrobials*, vol. 20, 2021, article 11. DOI: 10.1186/s12941-021-00417-y.

[23] Magiorakos, A.P. *et al.* "Multidrug-resistant, extensively drug-resistant and pandrug-resistant bacteria: An international expert proposal for interim standard definitions for acquired resistance." *Clinical Microbiology and Infection*, vol. 18, no. 3, 2012, pp. 268-281. DOI: 10.1111/j.1469-0691.2011.01470.x.

[24] Stepanović, S. *et al.* "Quantification of biofilm in microtiter plates: Overview of testing conditions and practical recommendations for assessment of biofilm production by staphylococci." *APMIS*, vol. 115, no. 8, 2007, pp. 891-899. DOI: 10.1111/j.1600-0463.2007.apm_630.x.

[25] Oh, H. *et al.* "Role of efflux pumps and mutations in genes for topoisomerases II and IV in fluoroquinolone-resistant *Pseudomonas aeruginosa* strains." *Microbial Drug Resistance*, vol. 9, no. 4, 2003, pp. 323-328. DOI: 10.1089/107662903322762743.

[26] La Rosa, R *et al.* "*Pseudomonas aeruginosa*: Persistence beyond antibiotic resistance." *Trends in Microbiology*, vol. 33, no. 10, 2025, pp. 1076-1084. DOI: 10.1016/j.tim.2025.05.004.

[27] Liang, Z. *et al.* "The role of individual exopolysaccharides in antibiotic tolerance of *Pseudomonas aeruginosa* aggregates." *Frontiers in Microbiology*, vol. 14, 2023, article 1187708. DOI: 10.3389/fmicb.2023.1187708.

[28] Valentin, J.D.P. *et al.* "Role of the flagellar hook in the structural development and antibiotic tolerance of *Pseudomonas aeruginosa* biofilms." *The ISME Journal*, vol. 16, no. 4, 2022, pp. 1176-1186. DOI: 10.1038/s41396-021-01157-9.

[29] Grandy, S. *et al.* "The identification of *Pseudomonas aeruginosa* persisters using flow cytometry." *Microbiology*, vol. 168, no. 10, 2022, article 001252. DOI: 10.1099/mic.0.001252.

[30] Pont, S. *et al.* "Intracellular *Pseudomonas aeruginosa* persist and evade antibiotic treatment in a wound infection model." *PLOS Pathogens*, vol. 21, no. 2, 2025, article e1012922. DOI: 10.1371/journal.ppat.1012922

[31] Shen, C. *et al.* "*Pseudomonas aeruginosa* tRNA nucleotidyltransferase Cca controls resistance and tolerance to aminoglycoside antibiotics by regulating the MexXY multidrug efflux pump." *Antimicrobial Agents and Chemotherapy*, vol. 70, no. 4, 2026, article e01653-25. DOI: 10.1128/aac.01653-25.

[32] Laborda, P. *et al.* "Mutations in the efflux pump regulator MexZ shift tissue colonization by *Pseudomonas aeruginosa* to a state of antibiotic tolerance." *Nature Communications*, vol. 15, 2024, article 2584. DOI: 10.1038/s41467-024-46938-w.

[33] Puja, H. *et al.* "The efflux pump MexXY/OprM contributes to the tolerance and acquired resistance of *Pseudomonas aeruginosa* to colistin." *Antimicrobial Agents and Chemotherapy*, vol. 64, no. 4, 2020, article e02033-19. DOI: 10.1128/AAC.02033-19.

[34] Kok, M. *et al.* "Nutrient conditions affect antimicrobial pharmacodynamics in *Pseudomonas aeruginosa*." *Microbiology Spectrum*, vol. 13, no. 1, 2025, article e01409-24. DOI: 10.1128/spectrum.01409-24.

[35] Meirelles, L.A. *et al.* "*Pseudomonas aeruginosa* faces a fitness trade-off between mucosal colonization and antibiotic tolerance during airway infection." *Nature Microbiology*, vol. 9, no. 12, 2024, pp. 3284-3303. DOI: 10.1038/s41564-024-01842-3.